Stratigraphy and Structure of the Dinkey Creek Roof Pendant in the Central Sierra Nevada, California

GEOLOGICAL SURVEY PROFESSIONAL PAPER 524-B

Stratigraphy and Structure of the Dinkey Creek Roof Pendant in the Central Sierra Nevada, California

By R. W. KISTLER *and* P. C. BATEMAN

SHORTER CONTRIBUTIONS TO GENERAL GEOLOGY

GEOLOGICAL SURVEY PROFESSIONAL PAPER 524-B

Multiple folding in the Dinkey Creek roof pendant of the central Sierra Nevada

UNITED STATES GOVERNMENT PRINTING OFFICE, WASHINGTON : 1966

UNITED STATES DEPARTMENT OF THE INTERIOR

STEWART L. UDALL, *Secretary*

GEOLOGICAL SURVEY

William T. Pecora, *Director*

For sale by the Superintendent of Documents, U.S. Government Printing Office
Washington, D.C. 20402

CONTENTS

	Page
Abstract	B1
Introduction	1
Bordering intrusive rocks	1
Formations	3
Gray marble	3
Calc-silicate rock	3
Lower member	3
Upper member	3
Biotite-andalusite hornfels	3
White quartzite	3
Schist	4
Formations—Continued	
Silicated marble, calc-silicate hornfels, and tactite inclusions in biotite-hornblende quartz monzonite	B4
Diorite sills and dikes	4
Structure	4
Structure diagrams	7
Initial orientation of the folds	7
Extent and cause of the deformations	11
Summary and conclusions	12
References cited	14

ILLUSTRATIONS

		Page
PLATE 1.	Geologic map, block diagram, and map showing metamorphic structures of the Dinkey Creek roof pendant, central Sierra Nevada, Calif	In pocket
FIGURE 1.	Generalized geologic map of the central Sierra Nevada	B2
2.	Crossbedding in white quartzite	4
3.	Typical first folds with cleavage parallel to axial surfaces	6
4.	Typical second fold in thin-bedded marble and hornfels	7
5.	Second fold in thin-bedded marble and hornfels	7
6.	Later folds crossing earlier folds in thin-bedded schist and quartzite	8
7.	Collective diagrams of structural elements in the Dinkey Creek roof pendant	9
8.	Subareas with a single cylindrical fold axis of bedding in the Dinkey Creek roof pendant	10
9.	Synoptic diagrams of first folds in the Dinkey Creek and Log Cabin roof pendants, Sierra Nevada, Calif	13

STRATIGRAPHY AND STRUCTURE OF THE DINKEY CREEK ROOF PENDANT IN THE CENTRAL SIERRA NEVADA, CALIFORNIA

By R. W. Kistler and P. C. Bateman

ABSTRACT

The Dinkey Creek roof pendant, about 50 miles northeast of Fresno in the central Sierra Nevada, Calif., is composed of a sequence of five sedimentary formations of Paleozoic or Mesozoic (pre-Cretaceous) age, which bordering plutons have thermally metamorphosed to the hornblende hornfels facies. During three successive tectonic episodes, three fold systems were formed. The first folds are overturned and have tightly appressed limbs; axial surfaces strike about N. 5° E. and dip 45° W. The second folds are open and have simple hinges; near-vertical axial surfaces strike about N. 20° W. The third folds are open and have simple hinges; near-vertical axial surfaces strike about N. 60° W. The deformations that produced the folds are thought to be regional because all three fold systems appear to have counterparts of similar style and axial surface orientation in other metamorphic remnants of the central Sierra Nevada.

INTRODUCTION

The Dinkey Creek roof pendant in the central Sierra Nevada, Calif., belongs to a belt of pendants composed chiefly of miogeosynclinal strata, which trend southeastward through the range for at least 100 miles—from near Huntington Lake at the north to Mineral King at the south (Bateman and others, 1963; Krauskopf, 1953). The distinctive lithologies of the formations, the presence of crossbeds in a quartzite formation, and a spectacular display of minor structural features in the Dinkey Creek roof pendant make it possible to determine the stratigraphy, geometry, and history of folding in rocks at the north end of this belt.

The pendant is in eastern Fresno County about 50 miles northeast of Fresno and 4 miles north of the Dinkey Creek resort area at an altitude of 7,600 to 9,700 feet (fig. 1). It underlies an area of about 8 square miles, but about 1 square mile in a long narrow curved septum at the southwest was not studied. The base for the geologic map of the pendant (pl. 1) is the manuscript compilation of the Huntington Lake 15-minute quadrangle, which is at a scale of 1:20,000. The scale has been reduced to 1:31,680 for publication. Most of the pendant is accessible by a good vehicle trail (four-wheel-drive road) that branches east from California State Highway 168 at Tamarack summit, about midway between Shaver Lake and Huntington Lake. The east end of the pendant can be reached by a very rough vehicle trail that runs northwest from the Dinkey Creek resort area.

The objectives of this study are (1) to determine the stratigraphic sequence of the strata in the roof pendant and the intrusive sequence of the plutons that border the pendant, (2) to determine the geometry and history of deformation of the pendant rocks, and (3) to determine whether the structural features in the pendant were caused by the emplacement of the bordering plutons and are confined to this pendant or whether they are represented in other metamorphic remnants and are of regional extent.

BORDERING INTRUSIVE ROCKS

The part of the pendant that was mapped is triangular shaped, and each side is in contact with different plutons of granitic rock (pl. 1). Hornblende-biotite granodiorite, "Dinkey Creek" type, lies along the northwest side; porphyritic biotite granite along the northeast side; garnet-bearing biotite granite along the west part of the south side; and biotite-hornblende quartz monzonite along the east part of the south side. Small masses of diorite of varied texture and composition, and older than either the hornblende-biotite granodiorite, "Dinkey Creek" type, or the porphyritic biotite granite, lie along the northeast side of the pendant. Designations of the plutonic rocks follow Krauskopf (1953). The biotite-hornblende quartz monzonite is, in fact, a complex of metamorphic and intrusive rocks, including diorite.

The sequence of intrusion is: (1) Diorite, (2) hornblende-biotite granodiorite, "Dinkey Creek" type, (3) porphyritic biotite granite and garnet-bearing biotite granite, and (4) biotite-hornblende quartz monzonite. The small masses of diorite along the northeast side of the pendant are intruded only by the porphyritic biotite granite and by the hornblende-biotite granodiorite, "Dinkey Creek" type. The porphyritic biotite granite and the garnet-bearing biotite granite both intrude the

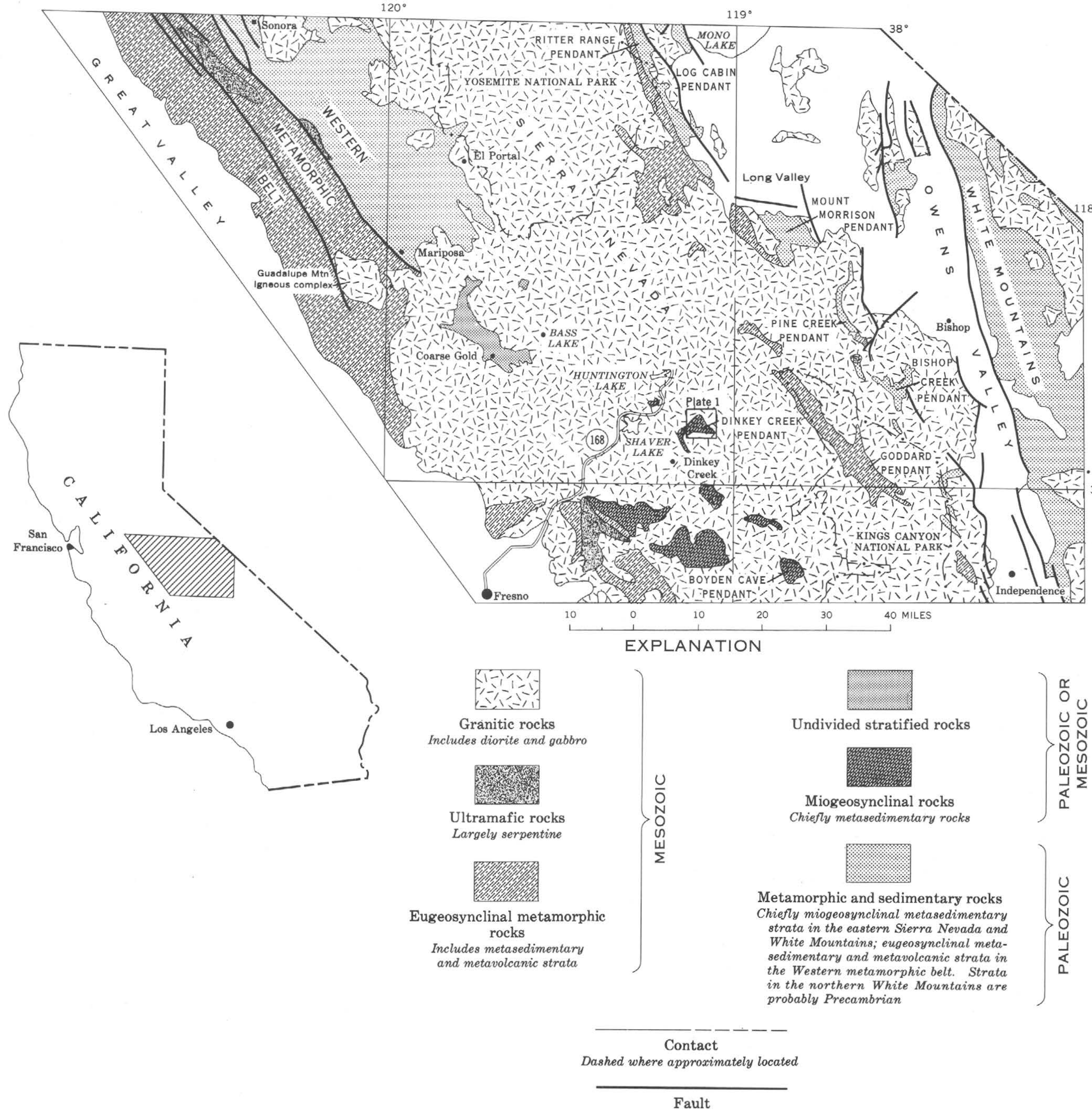

FIGURE 1.—Generalized geologic map of the central Sierra Nevada showing the location of the Dinkey Creek and other roof pendants.

hornblende-biotite granodiorite, "Dinkey Creek" type, and the biotite-hornblende quartz monzonite intrudes both the porphyritic granite and the hornblende-biotite granodiorite, "Dinkey Creek" type. The age relation of the biotite-hornblende quartz monzonite to the garnet-bearing biotite granite was not established, but the biotite-hornblende quartz monzonite is believed to be the older. Although the porphyritic biotite granite contains no garnet in the area shown on plate 1, it does contain garnet about 2 miles east of the pendant near Second Dinkey Lake; this fact suggests close relationship to the garnet-bearing biotite granite.

FORMATIONS

The pendant is composed of five formations of metamorphosed sedimentary rocks; it also contains a few dikes and sills of dark fine-grained diorite. The stratigraphic sequence from youngest to oldest is as follows:

5. Schist
4. White quartzite
3. Biotite-andalusite hornfels
2. Calc-silicate rock
1. Gray marble

These formations are lithologically distinctive, and all contacts between formations are sharp. The strata were derived from a sequence of calcareous, argillaceous, and arenaceous sediments that were deposited in a miogeosynclinal environment. Because most formations have been thickened by folding and thinned by attenuation of the less competent beds, original stratigraphic thicknesses cannot be determined with certainty. The entire exposed sequence may have had a stratigraphic thickness of only 3,000 to 4,000 feet. The stratigraphic thickness of the white quartzite formation may have been in the order of 1,500 to 2,000 feet, the biotite-andalusite hornfels 800 to 1,000 feet, and the calc-silicate rock about 200 feet; the gray marble and schist formations are incompletely exposed.

The mineral assemblages are compatible with the hornblende hornfels facies of thermal metamorphism (Fyfe and others, 1958, p. 205–211). Calcareous rocks are composed of various combinations of quartz, diopside, calcite, wollastonite, garnet, epidote, microcline, plagioclase, hornblende, and scapolite; pelitic rocks of combinations of quartz, muscovite, biotite, andalusite, and plagioclase; and quartzofeldspathic rocks of combinations of quartz, muscovite, biotite, microcline, and plagioclase.

Most rocks have a granoblastic texture, although a preferred orientation of micaceous minerals has persisted in some schistose specimens. Hornfels are generally equigranular and fine grained, but porphyroblasts of andalusite characterize the biotite-andalusite hornfels formation and argillaceous layers in the white quartzite and schist formations. Tactite adjacent to intrusive contacts and some calc-silicate rocks in the interior of the pendant are coarse grained.

GRAY MARBLE

The lowest exposed formation is finely laminated medium-gray marble. Individual laminae, generally an eighth of an inch or less in thickness, differ in grain size and shade. The formation is composed almost entirely of calcite and is probably clastic. Crossbeds appear to be present, but shears, parallel or subparallel to bedding, have a similar appearance to the crossbeds and make them unreliable for determining top directions. Small veins of white calcite, generally en echelon, are locally present.

CALC-SILICATE ROCK

This formation consists of two members separated by a sill of dark fine-grained diorite.

Lower member.—The part below the sill is a highly contorted sequence of interbedded marble, calc-silicate hornfels, and quartzofeldspathic hornfels. In outcrop, marble layers are buff to gray, and the calc-silicate hornfels layers are stained reddish brown by iron oxides. Individual layers are generally half an inch to several inches thick. Some layers of hornfels represent two or more layers that have been brought together by isoclinal folding or by the squeezing out of intervening marble layers.

Upper member.—The part above the sill consists of well-bedded buff marble and thin beds and lenses of greenish calc-silicate rock. Marble makes up at least 75 percent of the member. The calc-silicate rock is coarser grained than typical hornfels, and in places the layers are broken and boudined.

BIOTITE-ANDALUSITE HORNFELS

The biotite-andalusite hornfels formation is composed of remarkably uniform rock that is mottled light and dark gray. This mottling is on a scale of fractional parts of an inch and is caused by andalusite poikiloblasts. Originally the formation was an argillaceous shale or mudstone. Because the beds differ only slightly in composition and color, careful observation is required to identify bedding. In most outcrops the bedding is intricately contorted.

WHITE QUARTZITE

The most widespread unit in the pendant is composed chiefly of light-gray to buff quartzite, which is conspicuously crossbedded in many outcrops (fig. 2).

Within the quartzite are darker layers of pelitic hornfels, which comprise less than 5 percent of the formation. At the bottom of the formation and transitional to the underlying biotite-andalusite hornfels formation, is 10–15 feet of buff silicated marble and calc-silicate hornfels. Other calcareous layers and lenses are present within the quartzite, especially in the southeast end of the pendant where calcareous beds have been converted by contact metasomatism to scheelite-bearing tactite.

FIGURE 2.—Crossbedding in white quartzite. Beds are vertical; tops are to the right.

Crossbeds in the quartzite occur in layers that range from less than half an inch to more than a foot thick. Most crossbeds appear concave upward, but some appear linear and some sigmoid. Those that are concave upward were used to determine tops of beds. Quartz veins, commonly in gash systems arranged en echelon, are locally abundant. Deformation may obscure the crossbedding by producing, in areas of tight minor folds, shears that mimic the depositional structure. In determining top directions we have taken great care to ascertain that true crossbeds were being observed.

SCHIST

The stratigraphically highest unit in the pendant consists chiefly of thinly interbedded layers of very dark gray schist and light-gray to buff quartzite. Individual layers generally range in thickness from less than one-eighth of an inch to more than an inch. Crossbedded quartzite layers several feet thick are locally present. Also present are three layers composed of buff garnetiferous marble and buff to greenish calc-silicate hornfels which are shown separately on the geologic map.

The unit is one of the least competent in the pendant, and the original layering is strongly disrupted. Boudins and discontinuous lenses of quartzite are common; in places they parallel a secondary foliation transverse to the original bedding. Small-scale folds are conspicuous throughout the unit.

SILICATED MARBLE, CALC-SILICATE HORNFELS, AND TACTITE INCLUSIONS IN BIOTITE-HORNBLENDE QUARTZ MONZONITE

Small inclusions of silicated marble, calc-silicate hornfels, and tactite are scattered through a dark facies of the biotite-hornblende quartz monzonite. These inclusions cannot have come from the adjacent white quartzite but may have been carried upward by the quartz monzonite magma from the gray marble and calc-silicate rock formations. One of the inclusions is the site of the Garnet Dike tungsten mine.

DIORITE SILLS AND DIKES

Dark fine-grained diorite sills are present between the lower and upper members of the calc-silicate rock formation and within a calc-silicate hornfels member of the schist formation; a dike of similar rock cuts across the northernmost exposure of the gray marble and calc-silicate rock formations. These dikes and sills have been involved in the deformation of the enclosing sedimentary rocks and are doubtless older than any of the plutonic rocks.

STRUCTURE

The distribution of formations and the attitudes and top directions of beds indicate that the strata in the roof pendant have been complexly folded and thrust faulted. Three styles of folds were distinguished in the pendant, and their sequence established from the order of superimposition of folds of one style on another. The three generations of folds are designated first fold, second fold, and third fold.

The gross distribution of formations results chiefly from the first deformation when the largest folds in the pendant, an overturned anticline and companion syncline, were formed. Later folding has deformed these first folds, but the original attitude of their axial surfaces was probably very close to the present average attitude of those surfaces; their average strike is a little east of north, and their average dip is about 45° W. The large first folds are not obvious on the geologic map (pl. 1), mostly because related axial-plane faults complicate the structure, and glacial till obscures large parts of the structural pattern. The distribution of formations and bedding attitudes in the white quartzite clearly define the major first folds, however, and they are shown on the block diagram (pl. 1). The white quartzite formation is right-side-up along the northwest edge of the pendant, overturned in the middle part (just west of the schist), and right-side-up in the southeast part. In the north part of the pendant, the anticlinical hinge of the first fold is shown by the pattern of the biotite-andalusite hornfels, which wraps around the gray marble and the calc-silicate rock formations. The faulted hinge of the syncline is shown by the white quartzite, which wraps around the thin-bedded schist and quartzite formation in the south-central part of the pendant.

The axial beds of both the anticline and the syncline have been sheared out by thrust faults parallel with the axial surfaces and with bedding. The fault along the axial surface of the anticline is necessary to explain the absence of the calc-silicate rock formation from the northwestern limb of the anticline in the north part of the pendant and the absence of this formation and the underlying gray marble farther southwest along the projected trace of the axial surface. In the north end of the pendant, this fault must lie between the gray marble of the core and the biotite-andalusite hornfels of the northwestern limb of the anticline; farther southwest it probably follows the southeastern boundary of the biotite-andalusite hornfels on this northwestern limb (pl. 1). The fault along the axial surface of the syncline is required to explain the termination, downdip, of the three marble and calc hornfels beds in the schist formation against the white quartzite. A fault is also required in the eastern limb of the anticline between the white quartzite and the biotite-andalusite hornfels formations to explain the anomalous thinness of the overturned white quartzite west of the Rainbow tungsten mine. The faults have been folded with the first-generation folds and are believed to have developed during the later stages of first folding as an expression of extreme strain.

Complexes of minor folds that reflect the larger folds are common. First folds have tighly appressed limbs and simple hinges (fig. 3). Most minor first folds that were observed are of about the same scale as those shown in figure 3, but larger folds with amplitudes in the order of a few hundred feet are indicated by hinges and reversals in the top directions of beds. Less ductile beds generally have the same stratigraphic thicknessess everywhere in a fold, but more ductile beds have behaved plastically and thicken and thin irregularly—generally they are thicker in the apexes of folds and thinner on the limbs. First folds are like the composite folds of similar habit of Hills (1963, p. 234) and the quasi-flexural folds of Donath and Parker (1964, p. 59–60).

Major second-generation folds have substantially smaller amplitudes than the principal first folds and affect the gross distribution of formations correspondingly less than the first-generation structures. The axial surface of the first-generation syncline, for example, is only slightly deformed where crossed by the larger second folds. The axes and traces of axial surfaces of three second-generation folds are shown on the geologic map and block diagram (pl. 1). Minor second-generation folds have steep to vertical axial surfaces that strike about N. 20° W.; axes generally plunge 10°–25° northward, but steeper northward plunges have been observed, and gentle southward plunges occur in the southeast tip of the pendant. Second-generation folds are generally open and have simple hinges (figs. 4 and 5). They have the characteristics of folds formed by flexural slip or flexural flow (Donath and Parker, 1964, p. 51–55). Deformation of first-generation structural features by second folds is reflected in the gross distribution of the formations and in the relations of minor first and second folds to each other.

Third-generation folds were observed only locally in the roof pendant and are all minor. In places they are abundant and can be seen superimposed on first- and second-generation folds (fig. 6). Third-generation folds are open and have vertical axial planes that strike about N. 60° W.; fold axes plunge northwest. They are most conspicuous in the extreme northwest corner of the roof pendant.

Other structural elements in the roof pendant are cleavages and lineations (pl. 1). Cleavage occurs locally in association with all of the fold generations but is most commonly associated with first folds (fig. 3). Generally, it parallels or fans about axial surfaces. Much of the original cleavage was lost during metamorphism of the strata to the hornblende hornfels facies. Such cleavage as remains is pervasive and results from mineral orientation rather than from closely spaced fracture surfaces. In the biotite-andalusite hornfels, porphyroblasts of andalusite locally accentuate cleavage surfaces. Lineations other than minor folds in bedding are streaks of biotite and intersections of bedding and cleavage. All the lineations parallel fold axes.

796-523 O - 66 - 2

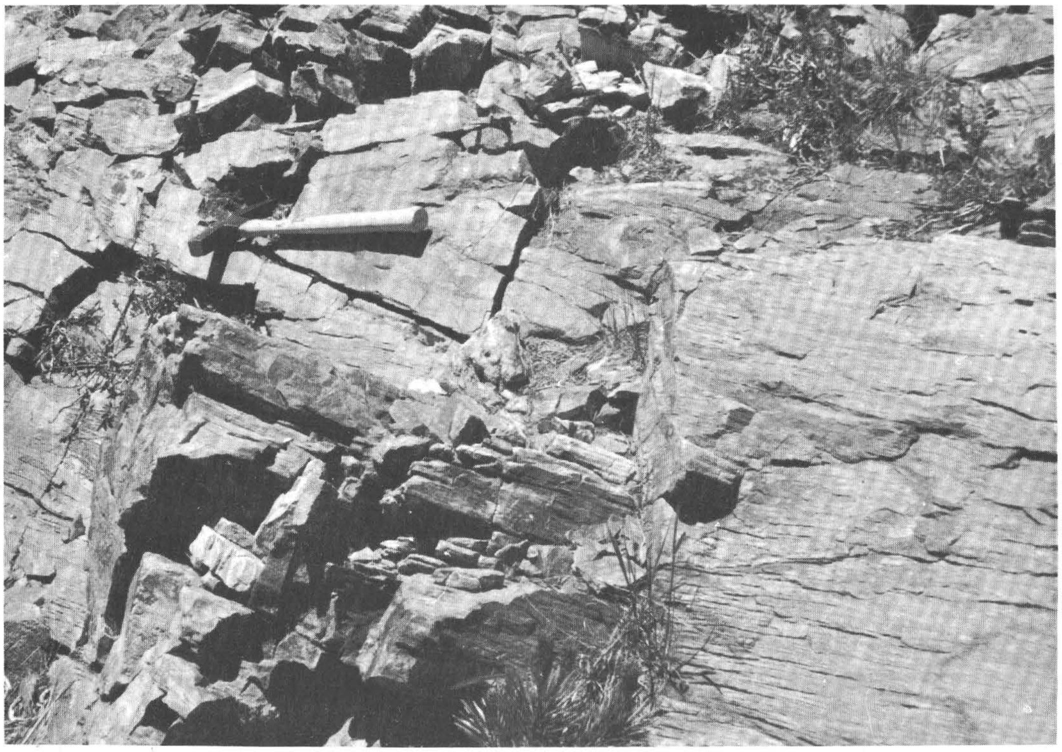

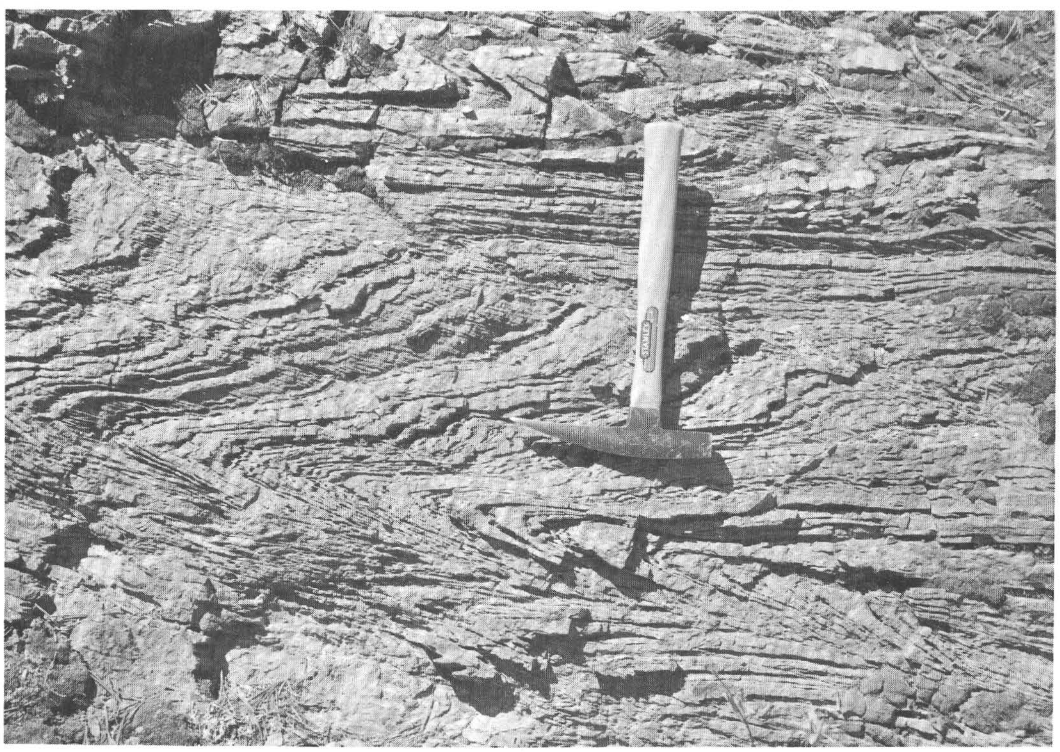

FIGURE 3.—Typical first folds with cleavage parallel to axial surfaces. *A* (upper), In thin-bedded schist and quartzite. *B* (lower), In thin-bedded marble and hornfels.

FIGURE 4.—Typical second fold in thin-bedded marble and hornfels.

FIGURE 5.—Second fold in thin-bedded marble and hornfels. Minor fold in limb (below hammer) may be either a first or second fold.

STRUCTURE DIAGRAMS

Collective diagrams for structural elements of the metamorphic rocks, plotted in lower hemisphere projections on an equal-area net, are as follows: Poles to bedding, poles to first-fold axial surfaces, first-fold axes, second- and third-fold axes, and lineations (fig. 7). The diagram showing poles to bedding (fig. 7*A*) indicates considerable dispersion about a rectalinear fold axis that plunges 25° N. 20° W. If small areas are removed at the two ends of the pendant, where field observations indicate the fold pattern is a little different than in the main body of the pendant, the dispersion around this axis is substantially reduced (fig. 8*B*). For convenience, we designate the south tip of the pendant, subarea 1; the main body of the pendant, subarea 2; and a small part of the north end, subarea 3 (fig. 8).

In subarea 1, poles to beds define a fold axis that plunges about 15° S. 25° E. (fig. 8*A*). Lineations in this subarea, mostly streaks of biotite on bedding surfaces, generally coincide with the fold axis defined by bedding attitudes. In the main part of the pendant, subarea 2, second-fold axes indicate a maximum (fig. 8*C*) that coincides with the fold axis normal to the girdle of poles to bedding (fig. 8*B*) and also with a fold axis normal to the partial girdle of poles to first-fold axial surfaces (fig. 8*D*). These relations show that this statistically defined rectilinear axis results from second folding; hence, we designate it β_2. First-fold axes in subarea 2 are rather widely scattered but generally plunge to the northwest (fig. 8*F*). In subarea 3, poles to bedding poorly define a fold axis that plunges west-northwest (fig. 8*G*). In this subarea both second- and third-fold axes are widely scattered.

INITIAL ORIENTATION OF THE FOLDS

The third folds are still in their original positions. Because third folds are too small for the structural elements of the second folds to have been significantly disturbed during their formation, we conclude that the second folds also are very close to their original positions. Field observations and the structural diagrams show that third-fold axial surfaces are near vertical and strike about N. 60° W. and that the fold axes plunge variably to the northwest. Second-fold axial surfaces also are near vertical and strike N. 20° W. In the main part of the pendant (subareas 2 and 3), second-fold axes plunge about 25° NW., but in the southeast end (subarea 1) they plunge 10–15° SE.

Because second folds are of considerable size, significant parts of the structural elements of the first folds must have been rotated during the formation of the second folds. The mechanism of second folding was by flexural slip or flexural flow; and the axis of second

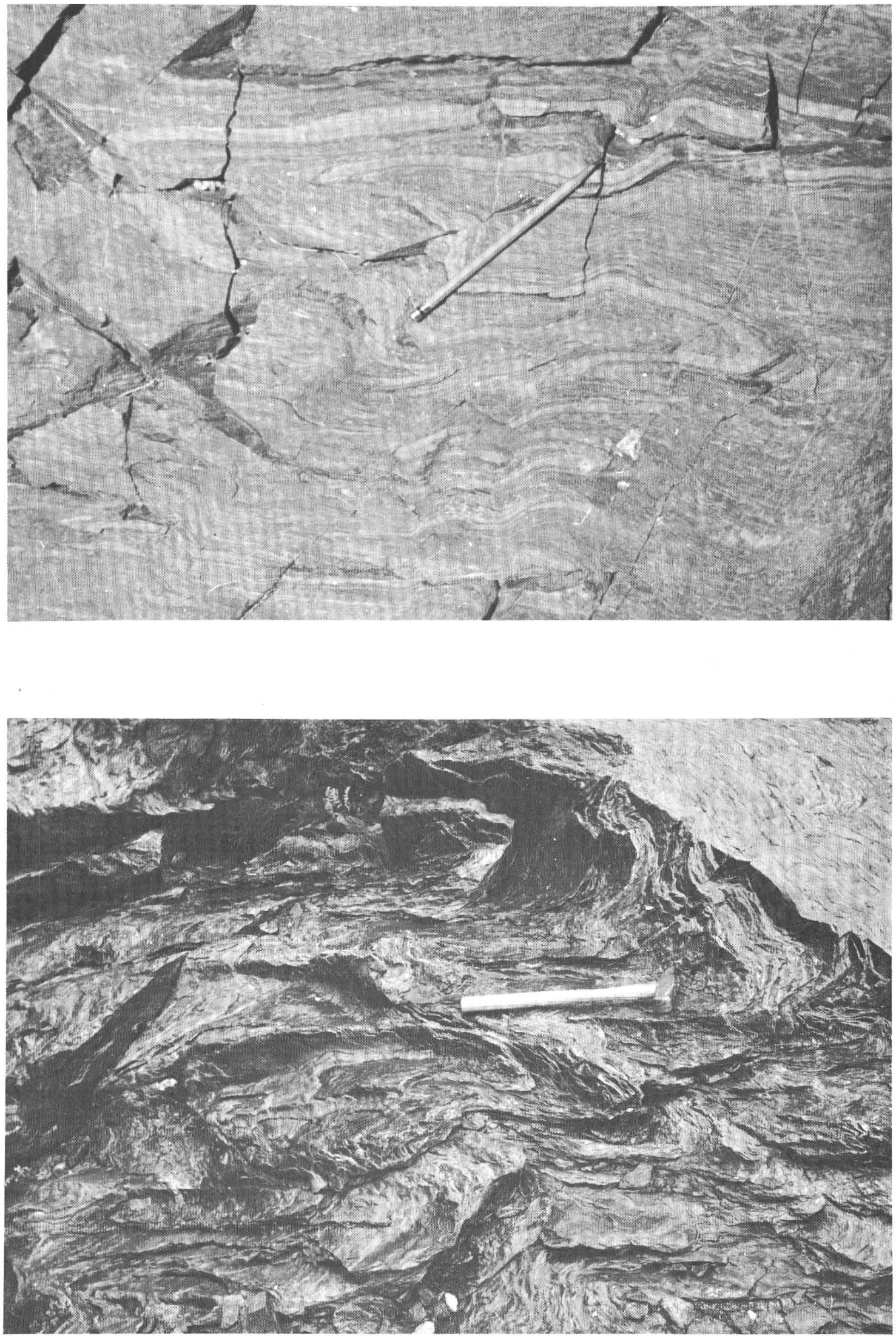

FIGURE 6.—Later folds crossing earlier folds in thin-bedded schist and quartzite. *A* (upper), Third fold (along pencil) crossing first folds. *B* (lower), Third folds superimposed on second folds. Second folds run from lower right to upper left; third folds run directly across photograph.

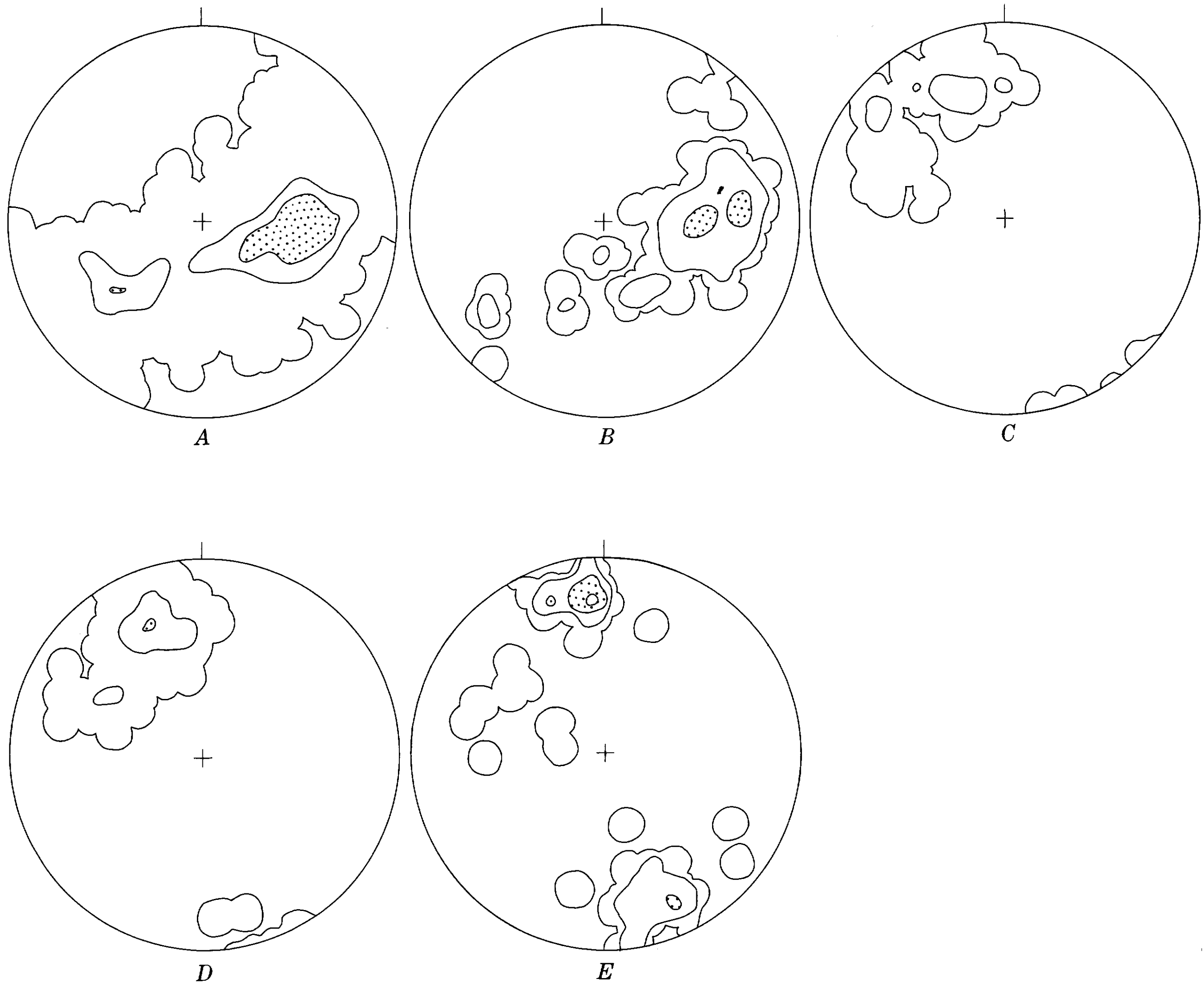

Diagram	Structural element	Points	Contours (percent per 1-percent area)
A	Poles to bedding	429	0. 23–2. 5–5
B	Poles to axial surface of first folds	70	1. 4–4. 3–10
C	First-fold axes	49	2–10
D	Second- and third-fold axes	101	1–10–20
E	Lineations (mineral streaks, bedding-cleavage intersection)	38	2. 7–10–18

FIGURE 7.—Collective diagrams of structural elements in the Dinkey Creek roof pendant.

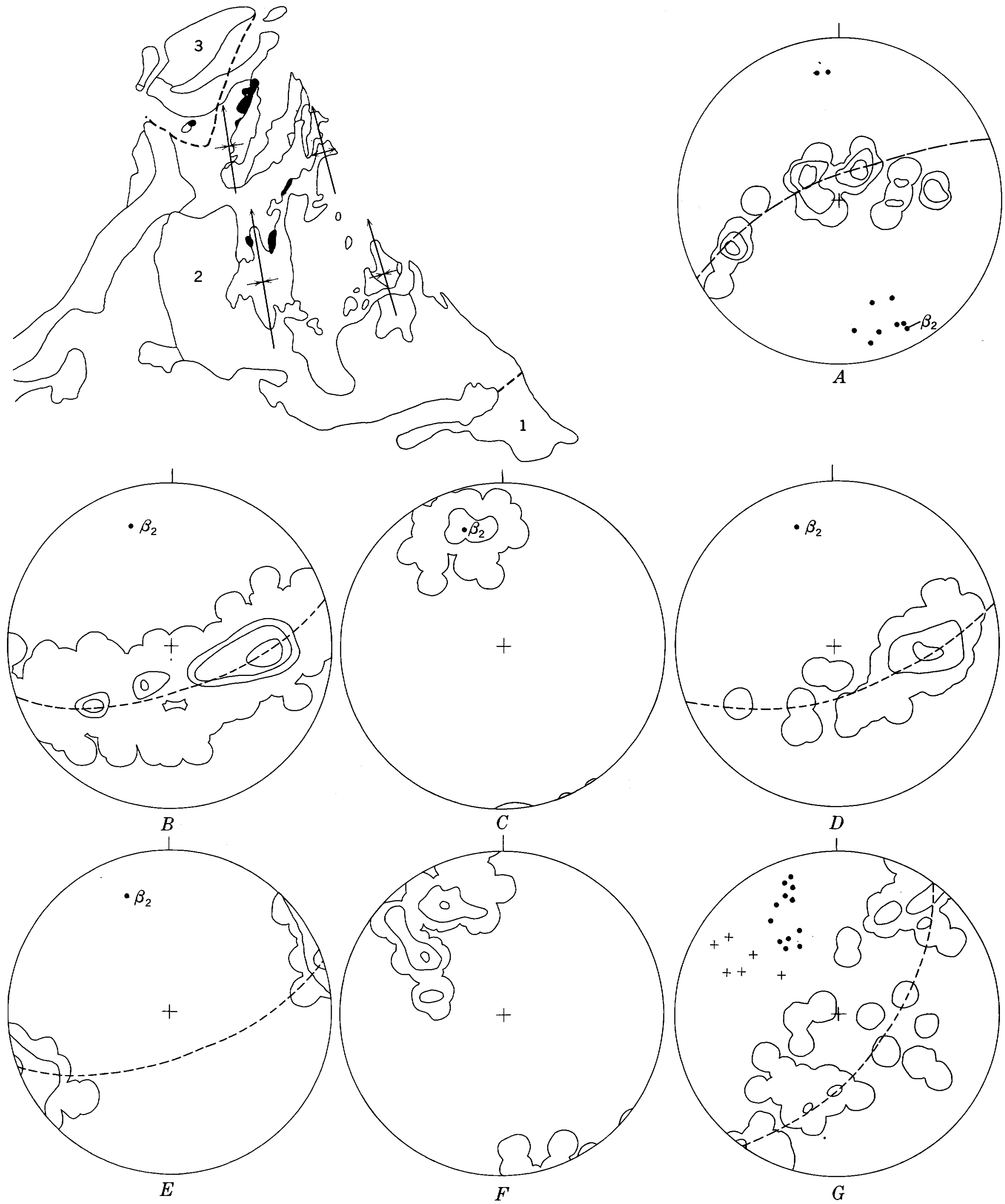

FIGURE 8.—Subareas with a single cylindrical fold axis of bedding in the Dinkey Creek roof pendant.

folding, β_2 = B_2 kinematic axis (Weiss, 1959, p. 92). When the second folds were formed, the structural elements of the first folds were rotated in planes or cones around β_2, depending on whether they were perpendicular or oblique to β_2. On structural diagrams they would plot respectively along a great circle and along small circles with β_2 at the center of the circles.

Coincidence of the two girdles formed by poles to first-fold axial surfaces (Fig. 8*D*) and poles to beds (fig. 8*B*) shows that the beds and axial surfaces of first folds are almost parallel and that therefore, first folds are isoclinal—a conclusion in agreement with field observations of nearly parallel bedding attitudes in right-side-up and overturned limbs of major first folds and of tightly appressed limbs of minor first folds.

Both of these girdles contain a principal maximum that plunges 40° S. 85° E. A question to consider is whether the maximum in the two girdles indicates the position of the poles to beds and first-fold axial surfaces prior to second folding, or whether it merely marks a preferred position into which the beds and first-fold axial surfaces were rotated during second folding. Field observations of minor second folds indicate that the second folding was not isoclinal; therefore, any maximum of poles to beds or to first-fold axial surfaces formed during second folding should occur in pairs at the ends of a partial girdle (Ramsay, 1964, fig. 10, p. 449). The fact that no other maximum in either girdle approaches the magnitude of the principal maximum shows that the principal maximum does not result from second folding and must represent the position of the poles to beds and first-fold axial surfaces prior to second folding.

If we look now at the diagram of first-fold axes (fig. 8F), it is evident that they do not lie on a small circle with a center at β_2; so, their present distribution could not have been caused by simple flexure folding about β_2 of first folds that had a very uniform axial orientation. The three maximums in the diagram lie close to, although not precisely along, a great circle whose pole plunges 40° N. 85° E.—very close to the maximum in the girdle of poles to bedding and to first-fold axial surfaces. Conceivably the distribution of the maximums could result from folds earlier than the presently recognized first folds, but as we observed no folds earlier than the first folds, it seems morelikely that the spread of maximums results from primary undulations of the first-fold axes in their axial surface. The axes scattered away from the great circle that passes through the three maximums probably result from rotation around β_2. According to this interpretation first-fold axial surfaces initially had a strike of N. 5° E. and a dip of 50° W. The fold axes pitched to the northwest in the axial surface at 30° to 80° (corresponding to plunges of 20° to 55°).

EXTENT AND CAUSE OF THE DEFORMATIONS

The deformed strata of the Dinkey Creek roof pendant provide no way to determine whether the successive deformations closely followed one another or were widely separated in time. Regional relations suggest, however, that the deformations were widely separated in time and that each fold system represents a distinct period of widespread regional deformation.

Two causes of the deformations can be envisaged: (1) The folds were caused by the emplacement of bordering plutons and are consequently limited to the pendant, and (2) the folds were caused by regional forces and are part of a regional pattern.

If the structural features in the metamorphic rocks were caused by the emplacement of bordering plutons, geometrical and temporal relations must exist between specific plutons and the different generations of folds. If all the folds were formed during one complex episode, the only intrusive in an orientation that could have produced the folds is the hornblende-biotite granodiorite ("Dinkey Creek" type). If the folds were formed during separate episodes, the most likely pairings are between the hornblende-biotite granodiorite ("Dinkey Creek" type) and first folds, between porphyritic biotite granite and second folds, and between the garnet-bearing biotite granite and third folds. The basis for these

EXPLANATION OF FIGURE 8

Subarea	Diagram	Structural element	Points	Contours (percent per 1-percent area)
1	*A*	Poles to bedding	24	4. 2–8. 3–12. 5
		• Lineations	9	Uncontoured
2	*B*	Poles to bedding	364	0. 35–4–5–10
	C	Second-fold axes	48	2. 1–20
	D	Poles to axial surfaces of first folds	58	1. 7–10–15
	E	Poles to axial surfaces of second folds	29	3. 2–10–33. 3
	F	First-fold axes	33	3. 3–10–20
3	*G*	Poles to bedding	45	2. 2–6. 6
		+ Third-fold axes	6	Uncontoured
		• Second-fold axes	12	Uncontoured

pairings is that these plutons could have been emplaced in the proper sequence, and their contacts with the pendant are subparallel with the fold systems with which they are paired. The fact that the fold systems appear to be regular and continuous throughout the pendant and to be truncated at its margins is a strong argument against relating the folds to the emplacement of the bordering plutons. The map pattern in the north part of the pendant suggests that second folds are truncated by the granodiorite ("Dinkey Creek" type). If so, both the first and second folds must be older than either the granodiorite or the porphyritic biotite granite.

The case for the folds having been caused by intrusion of the bordering plutons is thus very weak, but emplacement of plutons probably caused at least minor modifications of the structural features in the margins and at the ends of the pendant. In particular, the emplacement of plutons could have caused the structural variations in subareas 1 and 3 at the south and north ends of the pendant.

Comparison of structural features in the Dinkey Creek roof pendant with features determined in other roof pendants and in the southern part of the western metamorphic belt (fig. 1) suggests considerable correspondence of fold patterns. In the Log Cabin pendant, which lies directly west of Mono Lake, Kistler has identified, in Paleozoic rocks, folds similar in style and with axial surfaces parallel to the first folds of the Dinkey Creek pendant (fig. 9). In the northern extension of the Ritter Range pendant, Kistler has identified, in Paleozoic strata, first folds with axial surfaces that strike N. 10° W. and dip 45° W., second folds with vertical axial surfaces that strike N. 30° W., and third folds with vertical axial surfaces that strike N. 50° W. In this pendant, volcanic strata with a rubidium-strontium whole-rock age of 260 million years (C. E. Hedge, written commun., 1962) show no evidence of the first deformation and unconformably overlie Pennsylvanian-Permian(?) strata that were folded during the first deformation. These data suggest that the first deformation in the Ritter Range pendant must be Permian.

In the Goddard pendant we have identified first folds with nearly vertical axial surfaces that strike N. 25° W., parallel with the strata and oblique to the length of the pendant, and second folds with vertical axial surfaces that strike N. 50° W., parallel with the long axis of the pendant. In this pendant, small plutons of alaskite and granodiorite were emplaced after the first folding and were deformed during the second folding. In the southern part of the western metamorphic belt, the principal folds in the Upper Jurassic strata have axial surfaces that strike N. 45° W., and dip steeply east.

If the fold systems maintain their orientations (specifically, the orientations of their axial surfaces) across the width of the Sierra Nevada at this general latitude, the first folds in the Dinkey Creek pendant may correspond to the first folds in the Log Cabin pendant and northern extension of the Ritter Range pendant; the second folds to the second folds in the northern extension of the Ritter Range pendant and to the first folds in the Goddard pendant; and the third folds to third folds in the Ritter Range pendant, to second folds in the Goddard pendant, and to the regional folds in the southern part of the western metamorphic belt.

If we accept the correlation of the first deformation in the Dinkey Creek pendant with the first deformation in the Ritter Range pendant and the Permian age of the first deformation in the Ritter Range pendant, the strata in the Dinkey Creek pendant must be of Paleozoic age. In support of this conclusion is close resemblance of the strata of the Dinkey Creek pendant to strata of early Paleozoic age in the Mount Morrison pendant of the eastern Sierra Nevada (Rinehart and others, 1959). A Paleozoic age is in conflict with the tentative assignment of these strata to the Mesozoic, possibly the Triassic, made by Bateman and others (1963, p. D6) on the basis of lithologic correlation with the Boyden Cave pendant, 25 miles to the southeast, and with the Mineral King pendant, 60 miles to the southeast. Fossils of Triassic or Jurassic age have been collected from the Boyden Cave pendant (Moore and Dodge, 1962), and fossils of Late Triassic age have been collected from the Mineral King pendant (Knopf and Thelan, 1905; Durrell, 1940; Christensen, 1963). However, the facts that the strata in the Boyden Cave pendant, though lithologically similar to the strata in the Dinkey Creek pendant, do not seem to be stratigraphically equivalent and that the Mineral King pendant contains volcanic rocks and wackes in addition to miogeosynclinal strata leaves room for doubting the validity of the correlation. The strata in the Dinkey Creek pendant are lithologically unlike eugeosynclinal volcanic and sedimentary strata of Early Jurassic age in the Ritter Range pendant or of Late Jurassic age in the western metamorphic belt and are not likely to be Jurassic.

SUMMARY AND CONCLUSIONS

The Dinkey Creek roof pendant is composed of five metamorphosed sedimentary rock formations that have had the following history:

1. Depositions of calcareous, arenaceous, and argillaceous strata in a shallow marine environment.

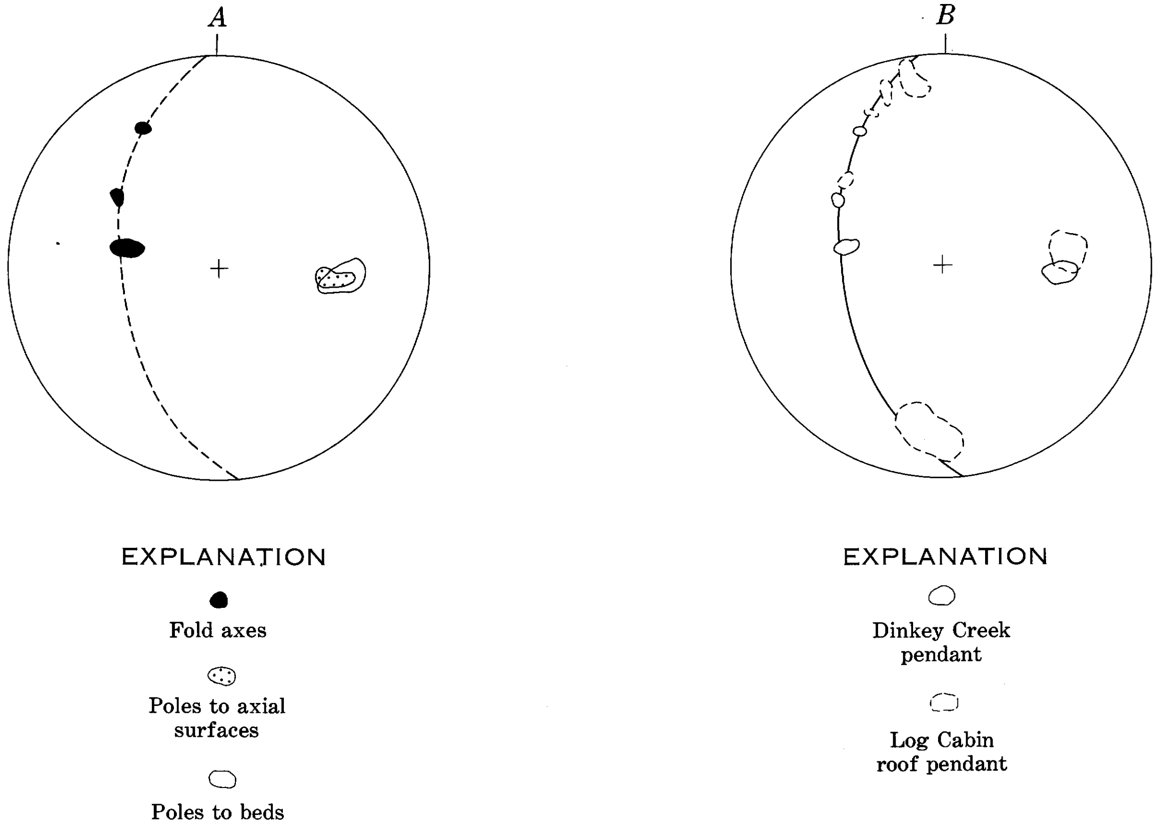

FIGURE 9.—*A*, Diagram of maximums of points representing first-fold axes, first-fold axial surfaces, and bedding in subarea 2, Dinkey Creek pendant. Note that the points abstracted from figures 8*B*, 8*D*, and 8*F* represent in projection an isoclinal fold with axial surface that strikes about north and dips about 45° W. Fold axes pitch at various angles to the northwest in the axial surface. *B*, Diagram showing maximums of first-fold axes and poles to axial surfaces in the Log Cabin roof pendant and in subarea 2 of the Dinkey Creek roof pendant. The interpreted original orientation of first-fold axial surfaces in the Dinkey Creek pendant closely approximates the measured attitude of first-fold axial surfaces in the Log Cabin roof pendant, which has not suffered major subsequent deformation. Note that in both pendants first-fold axes pitch at various angles in the first-fold axial surfaces.

2. Isoclinal folding with axial surfaces that strike N. 5° E. and dip 50° W. Thrust faulting following or contemporaneous with late stages of folding.
3. Open folding around vertical axial surfaces that strike about N. 20° W.
4. Minor folding around vertical axial surfaces that strike about N. 60° W.
5. Intrusion of the plutonic rocks and contact metamorphism of the sedimentary rocks to hornfels.

Comparison of the fold systems in the Dinkey Creek pendant with those of other pendants in the central Sierra Nevada suggests that the fold systems reflect regional deformations that were widely separated in time. The orientations of axial surfaces formed during each deformation seem to be remarkably constant over long distances. Such constancy may reflect deep burial of the strata at the time of folding with accompanying higher temperatures and greater pressures, which acted to reduce the contrast in structural competence of the different strata. If structural episodes can be correlated from roof pendant to roof pendant, age brackets can also be placed on strata that contain structural features formed during certain episodes. This technique would be especially useful as an aid to lithologic correlations in sparsely fossiliferous strata. However, much more detailed structural and stratigraphic work will be required before the validity of such correlations can be accepted without reservation.

REFERENCES CITED

Bateman, P. C., Clark, L. C., Huber, N. K., Moore, J. G., and Rinehart, C. D., 1963, The Sierra Nevada batholith—a synthesis of recent work across the central part: U.S. Geol. Survey Prof. Paper 414–D, p. D1–D46.

Christensen, M. N., 1963, Structure of metarmorphic rocks at Mineral King, California: California Univ. Pub. Geol. Sci., v. 42, no. 4, p. 159–198.

Donath, F. A., and Parker, R. B., 1964, Folds and folding: Geol. Soc. America Bull., v. 75, no. 1, p. 45–62.

Durrell, Cordell, 1940, Metamorphism in the southern Sierra Nevada northeast of Visalia, California: California Univ. Pub. Geol. Sci., v. 25, no. 1, p. 1–117.

Fyfe, W. S., Turner, F. J., and Verhoogen, Jean, 1958, Metamorphic reactions and metamorphic facies: Geol. Soc. America Mem. 73, 259 p.

Hills, E. S., 1963, Elements of structural geology: New York, John Wiley and Sons, Inc., 483 p.

Knopf, Adolph, and Thelan, Paul, 1905, Sketch of the geology of the Mineral King district, California: California Univ. Dept. Geology Bull., v. 4, p. 227–262.

Krauskopf, K. B., 1953, Tungsten deposits of Madera, Fresno, and Tulare Counties, California: California Div. Mines Spec. Rept. 35, 83 p.

Moore, J. G., and Dodge, F. C., 1962, Mesozoic age of metamorphic rocks in the Kings River area, southern Sierra Nevada, California, *in* Geological Survey Research 1962: U.S. Geol. Survey Prof. Paper 450–B, p. B19–B21.

Ramsay, J. G., 1964, The uses and limitations of beta-diagrams and pi-diagram in the geometrical analysis of folds: Geol. Soc. London Quart. Jour., v. 120, pt. 3, no. 479, p. 435–454.

Rinehart, C. D., Ross, D. C., and Huber, N. K., 1959, Paleozoic and Mesozoic fossils in a thick stratigraphic section in the eastern Sierra Nevada, California: Geol. Soc. America Bull., v. 70, no. 7, p. 941–945.

Weiss, L. E., 1959, Geometry of superposed folding: Geol. Soc. America Bull., v. 70, p. 91–106.